787

Resonance assignment of methionine methyl groups and χ^3 angular information from long-range proton–carbon and carbon–carbon J correlation in a calmodulin–peptide complex

Ad Bax, Frank Delaglio, Stephan Grzesiek and Geerten W. Vuister

Laboratory of Chemical Physics, National Institute of Diabetes and Digestive and Kidney Diseases,
National Institutes of Health, Bethesda, MD 20892, U.S.A.

SUMMARY

Several simple 3D experiments are used to provide J correlations between methionine C^ε methyl carbons and either the $C^\gamma H_2$ protons or C^β and C^γ. The intensity of the J correlations provides information on the size of the three-bond J couplings and thereby on the χ^3 torsion angle. In addition, a simple 3D version of the HMBC experiment provides a sensitive link between the $C^\varepsilon H_3$ methyl protons and C^γ. The methods are demonstrated for a 20 kDa complex between calmodulin and a 26-residue peptide fragment of skeletal muscle myosin light chain kinase.

INTRODUCTION

Calmodulin is a small regulatory protein which binds to more than two dozen different intracellular enzymes in a Ca^{2+}-dependent manner (Cohen and Klee, 1988). It is highly remarkable that a single protein can bind with high affinity to so many different targets. The structures of calmodulin complexed with three different target peptides have now been solved (Ikura et al., 1992; Meador et al., 1992,1993) and show that binding involves interaction between two hydrophobic patches located in the calmodulin C- and N-terminal domains and a peptide which adopts an α-helical conformation when bound. Target binding is calcium dependent, presumably because the hydrophobic patches are not accessible in the Ca^{2+}-free state (Kretsinger, 1992; Finn et al., 1994). The interaction between calmodulin and its target is largely hydrophobic in nature and, as suggested by O'Neil and DeGrado (1990), the unusually large number of methionine residues – eight out of nine are located in the two hydrophobic patches – is in part responsible for calmodulin's capability to bind to so many different targets. The long unbranched methionine
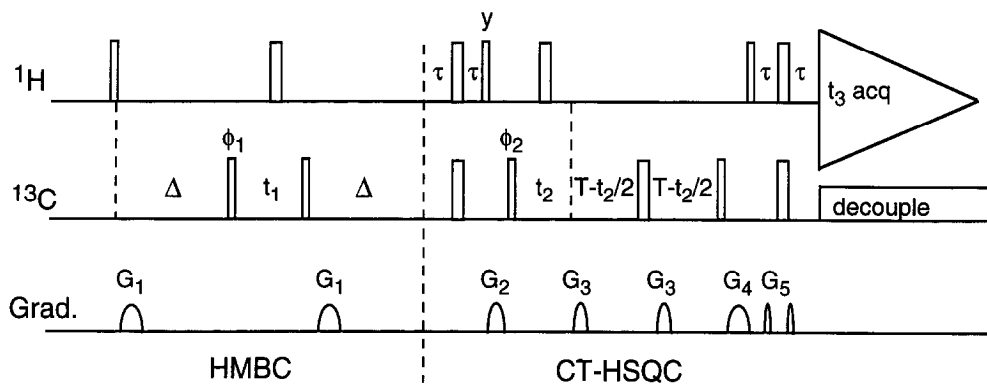
Fig. 1. Pulse scheme of the 3D HMBC experiment. Narrow rectangles correspond to pulses with a 90° flip angle, wide rectangles to 180°. Unless indicated otherwise, pulses are applied along the x axis. Delay durations: $\Delta = 28.4$ ms (optimized for $^1J_{C^\varepsilon H^\varepsilon} = 140.8$ Hz); $\tau = 1.75$ ms; $T = 7.5$ ms. $G_{1,2,3,4,5} = 1.6, 2.5, 0.5, 0.3$ and 0.1 ms. Phase cycling: $\phi_1 = x,-x$; $\phi_2 = x,x,-x,-x$; Receiver $= x,-x,-x,x$. Quadrature in the t_1 and t_2 dimensions is obtained by incrementing ϕ_1 and ϕ_2 in the regular States-TPPI manner (Marion et al., 1989).

side chain has a high degree of conformational freedom, which allows it to adapt its shape to that of the hydrophobic surface it is in contact with. Hence, methionine C^ε methyl groups play an essential role in target binding. For structure determination by NMR it is therefore important to obtain unambiguous assignments of these methyl groups. Moreover, as a decrease in entropy (associated with a rigidified side chain) lowers the binding affinity, it is interesting to see to what degree the side-chain mobility of methionines is restricted upon target binding.

If more than one methionine is present in a protein, their methyl groups are usually assigned on the basis of intraresidue NOEs in the NMR spectrum. In the case of calmodulin, this is not trivial, however, as two pairs of methionines (Met[71]/Met[72] and Met[144]/Met[145]) are in adjacent positions in the calmodulin sequence and many of the Met-C$^\gamma$H$_2$ resonances are poorly resolved. Although Ikura (1991, unpublished results) previously had managed to correctly assign seven of the nine methyl groups in the complex between calmodulin and a 26-residue peptide, based on a careful analysis of NOE spectra, assignments for Met[71] and Met[76] remained uncertain. The present study describes the use of three complementary 3D J correlation experiments, based on ^{13}C-^{13}C and ^{1}H-^{13}C long-range J couplings (Bax and Summers, 1986; Bax et al., 1992; Vuister et al., 1993), to obtain the methionine $C^\varepsilon H_3$ assignments. In addition, these experiments measure the size of the three-bond J couplings involved and thereby provide information on the χ^3 torsion angle.

Description of the pulse schemes

3D HMBC The pulse scheme for the 3D version of the HMBC experiments is shown in Fig. 1. In this experiment, magnetization is transferred as follows:

$$H^\varepsilon \rightarrow H^\varepsilon C^\gamma(MQ,t_1) \rightarrow H^\varepsilon \rightarrow C^\varepsilon(t_2) \rightarrow H^\varepsilon(t_3)$$
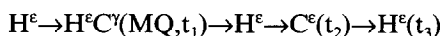
where MQ refers to heteronuclear H^ε-C^γ multiple-quantum coherence. This scheme yields a spectrum with correlations at coordinates $(F_1, F_2, F_3) = (\delta C^\gamma, \delta C^\varepsilon, \delta H^\varepsilon)$, where δC^γ, δC^ε and δH^ε are the chemical-shift frequencies of C^γ, C^ε and H^ε, respectively. The first part of the sequence
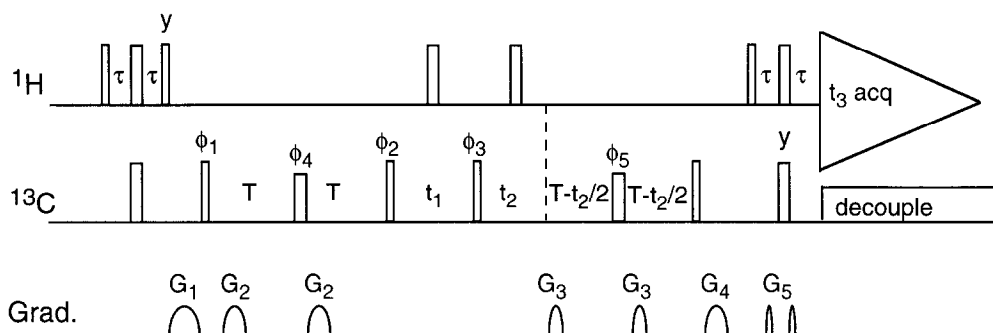
Fig. 2. Pulse scheme of the 3D LRCC experiment. Narrow rectangles correspond to pulses with a 90° flip angle, wide rectangles to 180°. Unless indicated otherwise, pulses are applied along the x axis. All pulses are applied at high power, except for the $180_{\phi4}$ and $180_{\phi5}$ ^{13}C pulses. Although not important for methionine methyl interactions, these pulses are adjusted to have a null in their excitation profile at the carbonyl frequency (τ_{180} = 46 μs at 151 MHz ^{13}C frequency; ^{13}C carrier at 42 ppm). Simultaneously with the 180° ^{1}H pulses applied at the midpoints of t_1 and t_2, 180° ^{15}N and ^{13}CO pulses (not shown) are applied in order to minimize J dephasing in the t_1 and t_2 dimensions for residues other than methionine. Delay durations: τ = 1.75 ms; T = 29 ms. $G_{1,2,3,4,5}$ = 2.5, 1.0, 0.4, 1.5 and 0.1 ms. Phase cycling: ϕ_1 = y,−y; ϕ_2 = x,x,−x,−x; ϕ_3 = 4(x),4(−x); ϕ_4 = x; ϕ_5 = 2(x),2(y),2(−x),2(−y); Receiver = x,−x,−x,x. Quadrature in the t_1 dimension is obtained by simultaneously incrementing ϕ_1, ϕ_4 and ϕ_2 in the regular States-TPPI manner, and in the t_2 dimension by incrementing ϕ_1, ϕ_4, ϕ_2 and ϕ_3.

corresponds to the original HMBC pulse scheme (Bax and Summers, 1986), but for uniformly ^{13}C-enriched proteins, the de- and rephasing delays, Δ, must be adjusted to an integer multiple of $1/^{1}J_{C^{\varepsilon}H}$ ($4/^{1}J_{C^{\varepsilon}H}$ or 28.4 ms in our case) to minimize generation of H^{ε}-C^{ε} multiple-quantum coherence. This stage is followed by a constant-time HSQC experiment (Santoro and King, 1992; Van de Ven and Philippens, 1992; Vuister and Bax, 1992), where the duration of the constant time, 2T, is adjusted to $1/(2\,^{1}J_{CC})$, 15 ms in practice. This choice for 2T acts as a methionine methyl filter, because the signal of all other carbons is greatly reduced by $^{1}J_{CC}$ dephasing.

^{13}C-^{13}C long-range correlation   The 3D version of the long-range ^{13}C-^{13}C (LRCC) correlation experiment (Bax et al., 1992) was adapted with pulsed field gradients to reduce the required phase cycling (Fig. 2). The changes relative to the original scheme are minor and only of a technical nature. A detailed description of the pulse scheme and the quantitation of J couplings is provided by Bax et al. (1992) and Vuister et al. (1994) and will not be repeated here. The LRCC experiment aims to correlate C^{ε} and H^{ε} with C^{β} (and C^{γ}). In the 2D version of this experiment, the H^{ε}-C^{β} correlations fall close to the intense 'diagonal' resonances of a multitude of H^{β}-C^{β} and H^{γ}-C^{γ} correlations of other residues, and therefore the present application requires the experiment to be performed in the 3D manner. In the LRCC scheme of Fig. 2, magnetization is transferred as follows:

$$H^{\varepsilon} \rightarrow C^{\varepsilon} \rightarrow C^{\varepsilon}/C^{\gamma}/C^{\beta}(t_1) \rightarrow C^{\varepsilon}(t_2) \rightarrow H^{\varepsilon}(t_3)$$
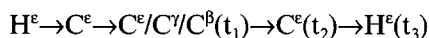
and resonances in the 3D spectrum appear at $(F_1,F_2,F_3) = (\delta C^{\varepsilon}/\delta C^{\gamma}/\delta C^{\beta}, \delta C^{\varepsilon}, \delta H^{\varepsilon})$. Thus, during the t_1 evolution period, three different types of magnetization evolve: C^{ε} magnetization which has not dephased with respect to C^{γ} or C^{β} during the preceding period 2T, and C^{γ} and C^{β} magnetization (antiphase with respect to C^{ε}), transferred from C^{ε} by the $90°_{\phi2}$ ^{13}C pulse. In principle, the $90°_{\phi2}$ pulse also generates $C^{\varepsilon}C^{\gamma}C^{\beta}$ three-spin coherence, but this fraction is negligible as its
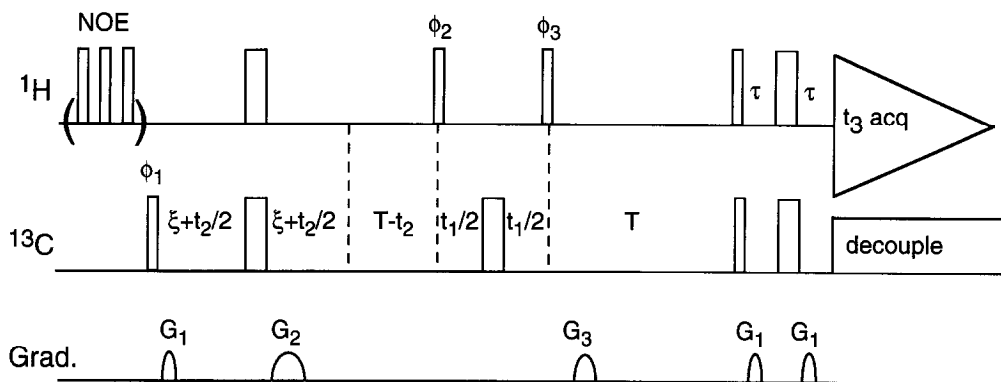
Fig. 3. Pulse scheme of the 3D LRCH experiment. Narrow rectangles correspond to pulses with a 90° flip angle, wide rectangles to 180°. Unless indicated otherwise, pulses are applied along the x axis. During the 700 ms delay between scans, 120° proton pulses, separated by 10 ms intervals, are used for obtaining NOE enhancement of the $^{13}C^\varepsilon$ methyl magnetization. Delay durations: ξ = 0.9 ms, τ = 1.75 ms; T = 19.6 ms. $G_{1,2,3}$ = 0.3, 0.8 and 0.5 ms. Phase cycling: ϕ_1 = y,−y; ϕ_2 = x,x,−x,−x; ϕ_3 = 4(x),4(−x); Receiver = x,−x,−x,x,−x,x,x,−x. For the 2D reference spectrum, t_1 is kept at 2 μs, and Receiver = x,−x, with phase cycling for ϕ_1, ϕ_2 and ϕ_3 the same as for the 3D experiment. Quadrature in the t_1 and t_2 dimensions is obtained by incrementing ϕ_2 and ϕ_1 in the regular States-TPPI manner.

amplitude is proportional to $\sin(2\pi J_{C^\varepsilon C^\gamma} T)\sin(2\pi J_{C^\varepsilon C^\beta}T)$, whereas the antiphase C^γ and C^β components during t_1 are proportional to $\sin(2\pi J_{C^\varepsilon C^\gamma} T)$ and $\sin(2\pi J_{C^\varepsilon C^\beta} T)$, respectively. The ratio of the integrated cross-peak intensity, caused by the long-range coupling of size ^nJ, versus the 'diagonal' C^ε intensity in this experiment depends on $\tan^2(2\pi^nJT)$ (Bax et al., 1992; Vuister et al., 1994). Measurement with 2T = 28 ms indicated that a number of the two- and three-bond $J_{C^\varepsilon C^\gamma}$ and $J_{C^\varepsilon C^\beta}$ couplings were smaller than ~0.7 Hz, i.e., too small to yield observable cross-peak intensity. For many of the methionines, this situation improves when using a very long duration, 2T = 56 ms, for the de- and rephasing intervals. Note that for measuring J_{CC} couplings to methionine C^ε the de/rephasing period 2T does not need to be set to an integral multiple of $1/^1J_{CC}$, but this choice also allows measurement of $^nJ_{CC}$ for residues other than methionine from the same 3D spectrum.

C^ε-H^γ *J correlation* In the long-range ^{13}C-^{1}H (LRCH) experiment (Fig. 3), magnetization is transferred as follows:

$$C^\varepsilon(t_2) \rightarrow C^\varepsilon H^\gamma(MQ,t_1) \rightarrow C^\varepsilon \rightarrow H^\varepsilon(t_3).$$

This results in correlations at frequency coordinates $(F_1,F_2,F_3) = (\delta H^\gamma, \delta C^\varepsilon, \delta H^\varepsilon)$. Spurious diagonal peaks occur at $(F_1,F_2,F_3) = (\delta H^\varepsilon, \delta C^\varepsilon, \delta H^\varepsilon)$. Two slightly different schemes have been proposed previously for obtaining this type of data. A method for selectively ^{13}C-labeled proteins was demonstrated for $^{13}C^\delta$-leucine-labeled staphylococcal nuclease (Vuister et al., 1993) and a modified version of this experiment has been demonstrated on uniformly ^{13}C-labeled proteins. The latter method (Vuister and Bax, 1993) is somewhat less sensitive, as additional care needs to be taken to avoid dephasing due to $^1J_{CC}$. However, the $^{13}C^\varepsilon$ of methionine is not subject to $^1J_{CC}$ coupling and the original and more sensitive method of Vuister et al. (1993) therefore was used instead. This scheme has been modified slightly, as shown in Fig. 3, by omitting one ^{1}H 180° pulse and by inserting pulsed field gradients for reducing the required phase cycle. For $2\xi + T = n/J_{C^\varepsilon H^\varepsilon}$ and $2\xi + T \ll 1/J_{C^\varepsilon H^\gamma}$, the C^ε-H^γ correlation intensity in this experiment is, to a first approxim-

ation, proportional to $\sin[\pi(2\xi + T)J_{C^\epsilon H^\gamma}]\sin(\pi T J_{C^\epsilon H^\gamma}) \approx \sin^2[\pi(\xi + T)J_{C^\epsilon H^\gamma}]$ (Vuister et al., 1993), whereas the intensity of spurious C^ϵ-H^ϵ correlations in this spectrum is proportional to $3\sin[\pi(2\xi + T)J_{C^\epsilon H^\epsilon}]\sin(\pi T J_{C^\epsilon H^\epsilon})\cos^2(\pi T J_{C^\epsilon H^\epsilon}) \approx \sin[\pi(2\xi + T)J_{C^\epsilon H^\epsilon}]$. Hence, even very small deviations from the desired condition, $2\xi + T = n/J_{C^\epsilon H^\epsilon}$, can cause significant spurious intensity for the C^ϵ-H^ϵ correlation in the 3D LRCH spectrum. As described by Vuister et al. (1993), quantitative information on $J_{C^\epsilon H^\gamma}$ can be obtained from the relative intensities in a 2D reference spectrum and the long-range correlations in the 3D spectrum.

EXPERIMENTAL

All experiments were carried out on a Bruker AMX-600 spectrometer, equipped with a triple-resonance self-shielded z gradient probehead and a SIG-MAX™ ¹H preamplifier. All field gradient pulses have a sine-bell shape, with a maximum gradient of 25 G/cm at the center of the sine bell. Gradient currents were generated by an inexpensive in-house built gradient-shaping and amplifier unit (Tschudin, R., unpublished results). In all experiments, pulsed field gradients were used to reduce the need for extensive phase cycling, without affecting the inherent sensitivity (Bax and Pochapsky, 1992).

The NMR sample consisted of genetically engineered uniformly ^{13}C-/^{15}N-enriched *Drosophila* calmodulin, lacking the posttranslational modifications present in natural calmodulin. The protein was complexed with one equivalent of the synthesized peptide KRRWKKNFIAV-SAANRFKKISSSGAL, commonly known as M13 (Klevit et al., 1984), and 4 molar equivalents of Ca^{2+}. The concentration of the complex was 1.0 mM in 99.5% D_2O, 100 mM KCl, pH 6.8 (uncorrected meter reading). All experiments were carried out at 35 °C. Details regarding data acquisition and processing are given below. Relevant pulse widths and delay durations used in the various pulse schemes are provided in the legends to Figs. 1–3.

3D HMBC

The spectrum results from a 64* × 20* × 512* acquired data matrix with spectral widths of 70.5 ppm (^{13}C, F_1), 10 ppm (^{13}C, F_2) and 10 ppm (^{1}H, F_3), using the pulse scheme of Fig. 1. Data have been mirror-image linear predicted (Zhu and Bax, 1990) in the constant-time t_2 dimension and apodized by 66°-shifted squared sine-bell windows in all three dimensions. Time-domain data have been zero-filled to yield digital resolutions of 0.55 ppm (F_1), 0.08 ppm (F_2) and 0.005 ppm (F_3). Data have been acquired using 32 scans per hypercomplex $t_1/t_2/t_3$ increment, i.e., eight transients were co-added. The total acquisition time was 10 h. The 2D spectrum of Fig. 4 also has been acquired using the scheme of Fig. 1, but keeping t_2 at zero, and Δ adjusted to 3.4 ms for generating one-bond H^ϵ-C^ϵ instead of three-bond H^ϵ-C^γ multiple-quantum coherence. This spectrum results from a 100* × 512* data matrix with four scans per complex t_1/t_3 increment and spectral widths of 33 ppm (F_1) and 10 ppm (F_3). The total acquisition time was 6 min.

3D LRCC

The spectrum results from a 120* × 38* × 512* acquired data matrix with spectral widths of 70.5 ppm (^{13}C, F_1), 10 ppm (^{13}C, F_2) and 10 ppm (^{1}H, F_3), using the pulse scheme of Fig. 2. Data were mirror-image linear predicted in the constant-time t_2 dimension and apodized by 80°-shifted

squared sine-bell windows in all three dimensions. Time-domain data have been zero-filled to yield digital resolutions of 0.55 ppm (F_1), 0.08 ppm (F_2) and 0.005 ppm (F_3). Data have been acquired using 48 scans per hypercomplex $t_1/t_2/t_3$ increment, i.e., 12 transients were co-averaged. The total measuring time was 48 h.

3D LRCH

The spectrum results from a 64* × 60* × 512* acquired data matrix with spectral widths of 6.66 ppm (^{1}H, F_1), 10 ppm (^{13}C, F_2) and 10 ppm (^{1}H, F_3), using the pulse scheme of Fig. 3. Data were mirror-image linear predicted in the constant-time t_2 dimension and apodized by cosine-squared windows in all three dimensions. Time-domain data were zero-filled to yield digital resolutions of 0.05 ppm (F_1), 0.08 ppm (F_2) and 0.005 ppm (F_3). Data were acquired using 32 scans per hypercomplex $t_1/t_2/t_3$ increment, i.e., eight transients were co-averaged. The total acquisition time was 36 h. Except for the constant $t_1 = 0$ duration and the different phase cycling used, the 2D (F_2/F_3) reference spectrum was acquired and processed identically to the 3D spectrum, using 16 scans per complex t_2/t_3 increment, i.e., again co-adding eight transients. The signal amplitudes in the 2D and 3D spectra were obtained by iterative nonlinear least-squares peak fitting (Delaglio, F., unpublished results), which is slightly less sensitive to random noise than straightforward volume integration. The fitting procedure uses model line shapes derived from Fourier-transformed time-domain signals, thus automatically compensating for scaling that occurs during Fourier transformation of the experimental data.

RESULTS AND DISCUSSION

Figure 4 shows the ^{1}H$^\varepsilon$-^{13}C$^\varepsilon$-filtered correlations for the nine methionine residues in calmodulin, recorded with the scheme of Fig. 1. Met[76] shows two minor components (~25% and ~5% intensity) immediately adjacent to its main resonance in the ^{1}H-^{13}C correlation spectrum. This residue is located in the highly flexible linker region between the N- and C-terminal domains of calmodulin. The origin of this heterogeneity existing in the vicinity of Met[76], which was also observed in some of our earlier studies, has not yet been established. The C$^\varepsilon$H$_3$ resonances for Met[124] and Met[145] are considerably weaker than for the remainder of the C$^\varepsilon$H$_3$ groups. Their
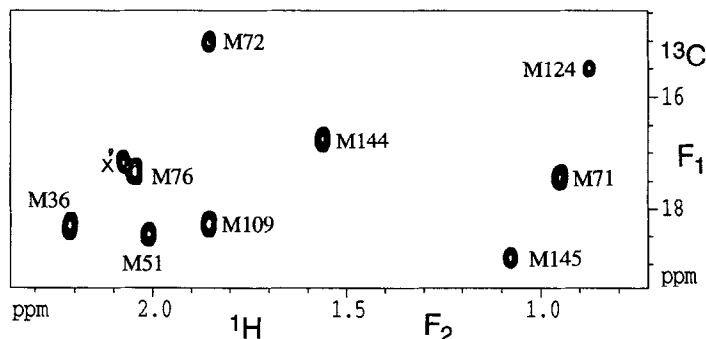
Fig. 4. Methionine-edited ^{1}H$^\varepsilon$-^{13}C$^\varepsilon$ correlation spectrum of the calmodulin–M13 complex, recorded with the scheme of Fig. 1, using $\Delta = 3.4$ ms (for optimizing generation of one-bond instead of three-bond ^{1}H-^{13}C coherence) and keeping $t_2 = 0$. Chemical shifts are relative to TSP. 'x' marks the 'diagonal' C$^\varepsilon$H$_3$ resonance of a minor component of Met[76].
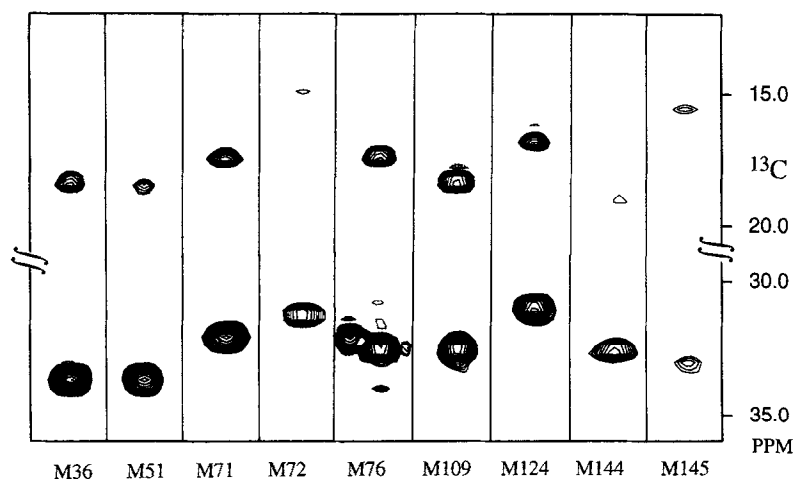
Fig. 5. F_1 strip plot of the 3D HMBC spectrum of the calmodulin–M13 complex, showing the correlation between C^ϵ/H^ϵ and C^γ, plus spurious 'diagonal' ($F_1 = F_2 = \delta C^\epsilon$) resonances for C^ϵ-H^ϵ. Contours are spaced exponentially by $2^{1/3}$.

intensity rapidly decreases when the temperature is lowered below 35 °C, suggesting that their environment in the protein is time-dependent on a time scale of micro- to milliseconds.

Figure 5 shows the result of using the 3D HMBC experiment for obtaining information on long-range connectivities between the C^ϵ methyl group and C^γ. The HMBC correlations to C^γ caused by the $^3J_{H^\epsilon C^\gamma}$ coupling (~5 Hz) are quite intense and, except for Met[145], all could be observed in the first t_1/t_3 plane ($t_2 = 0$), i.e., they were observable within 15 min of data acquisition. A complete set of strips, taken from the 3D spectrum, is shown in Fig. 5. The resonance for Met[145] is very weak, due to its short $^1H^\epsilon$ T_2 and the relatively long values used for the HMBC delays Δ. As can be seen from Fig. 5, several of the C^γ resonances are pairwise degenerate and even if previous assignments for C^γ had been complete, not all $C^\epsilon H_3$ groups could be assigned on the basis of this spectrum. In contrast, all $^{13}C^\beta$ resonances previously have been assigned by 3D HCCH techniques (Bax et al., 1990; Fesik et al., 1990; Kay et al., 1990) and by CBCACONH and CBCANH experiments (Grzesiek et al., 1992), and all have unique C^β chemical shifts.

Figure 6 shows F_1 strips of the LRCC 3D spectrum, including both the intense 'diagonal' methionine C^ϵ resonance (in the 15–20 ppm region) and the much weaker long-range correlations to C^β and C^γ, which correspond to magnetization that has been transferred from C^ϵ to C^β/C^γ during t_1 and back to C^ϵ. The 'diagonal' $^{13}C^\epsilon$ methyl resonances correspond to magnetization that has not been transferred to $^{13}C^\beta$ or $^{13}C^\gamma$. Contours for these diagonal resonances are plotted at a level that is 10 times higher compared to the cross peaks in the 29–34 ppm region. Met[36], Met[72] and Met[76] show resolved correlations to both C^β and C^γ. The C^γ resonance is immediately identified on the basis of the HMBC spectrum of Fig. 5. As discussed previously (Bax et al., 1992; Vuister et al., 1994), the intensity ratio of the cross and diagonal peaks, to a good approximation, equals $\tan^2(2\pi J_{lr}T)$, where J_{lr} is the size of the long-range ^{13}C-^{13}C J coupling. Quantitative analysis of the two-bond correlation intensity yields $^2J_{CC}$ values in the 0.5–0.6 Hz range. Considering the absence of electronegative substituents on C^γ (except for sulfur, which is in the coupling pathway), $^2J_{C^\epsilon C^\gamma}$ is expected to be largely independent of the χ^3 torsion angle. For most other methionine residues, C^β and C^γ resonances are unresolved. However, the cross-peak positions observed for
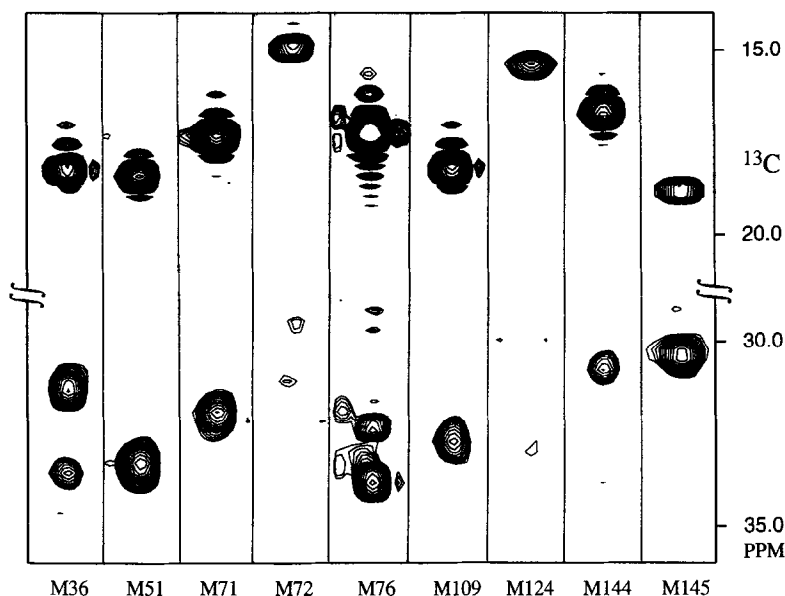
Fig. 6. F_1 strip plot of the 3D LRCC spectrum of the calmodulin–M13 complex, showing the correlations between $C^\varepsilon/H^\varepsilon$ and C^β and C^γ resonances for the methionine residues. The lowest contour level for the 'diagonal' ($F_1 = F_2$) peaks is 10 times higher than for the cross peaks (in the 29–34 ppm region). Diagonal and cross peaks have opposite phase. Contours are spaced exponentially by $2^{1/3}$.

Met[51] and Met[71] agree better with the $^{13}C^\beta$ chemical shifts, previously determined from the CBCACONH experiment, than with the C^γ shifts determined from the above described HMBC experiment. This indicates that for these two residues the correlation is dominated by $^3J_{C^\beta C^\varepsilon}$. Approximate values for $^3J_{C^\beta C^\varepsilon}$ can be obtained by subtracting from the integrated cross-peak intensity the intensity that is expected for a 0.5 Hz value of $^2J_{C^\gamma C^\varepsilon}$ (Table 1). For Met[109], Met[124] and Met[144] the cross-peak/diagonal-peak intensity ratios are very low, indicative of very small (~0.5 Hz) values for both $^3J_{C^\beta C^\varepsilon}$ and $^2J_{C^\gamma C^\varepsilon}$.

Except for Met[72] and Met[124], the diagonal/cross-peak intensity ratios measured for the spectrum of Fig. 6 all agree within 16% with values measured from a less sensitive LRCC spectrum, recorded by using 2T = 29 ms (data not shown), but otherwise identical conditions. Considering that $\tan(2\pi J_{lr}T) \ll 1$, an error of 16% in the intensity ratio corresponds to an error of only ~8% in the measured coupling, and the random error in the derived J_{CC} values is therefore believed to be smaller than a few tenths of a hertz. In addition to the random error caused by uncertainties in the intensities, a systematic error may be introduced by pulse imperfections, which will reduce the cross/diagonal-peak intensity ratios and result in systematic underestimation of the J_{CC} values by as much as 6% (Zhu and Bax, 1993).

Considering that Met[76] is located near the middle of a long and flexible solvent-exposed loop, it seems reasonable to assume that the 0.8 and 0.5 Hz $^3J_{C^\beta C^\varepsilon}$ and $^2J_{C^\gamma C^\varepsilon}$ values correspond to those of a fully flexible methionine residue, with all three χ^3 rotamers significantly populated. For two of the residues, Met[51] and Met[145], the $^3J_{C^\beta C^\varepsilon}$ coupling is found to be significantly larger than for the remainder of the methionines, suggesting a high occupation of the $\chi^3 = 180°$ rotamer; Met[72], Met[109], Met[124] and Met[144] exhibit smaller than average $^3J_{C^\beta C^\varepsilon}$ values, suggestive of a more than

average population of the $\chi^3 = \pm 60°$ conformers.

Further information on the χ^3 angle is obtained from the measurement of $^3J_{C^\varepsilon H^\gamma}$. For a 180° χ^3 angle, both $^3J_{C^\varepsilon H^\gamma}$ couplings are gauche, and small values are expected. For $\chi^3 = \pm 60°$, the coupling to one of the H^γ protons is expected to be large, whereas $^3J_{C^\varepsilon H^\gamma}$ to the second one remains small. As discussed previously (Vuister et al., 1993), ^1H-^1H spin flips during the de- and rephasing delays, T + 2ξ and T, result in measured $^3J_{C^\varepsilon H^\gamma}$ values that are smaller and larger than the true values for the larger and the smaller of the two $^3J_{C^\varepsilon H^\gamma}$ couplings, respectively. Under the conditions of the present experiment, the difference between the two couplings is expected to be attenuated by less than 20% (Vuister et al., 1993).

A plot showing F_1 strips of the long-range C^ε-H^γ correlation spectrum is shown in Fig. 7. Spurious correlations via $^1J_{C^\varepsilon H^\varepsilon}$ are also observed in this spectrum, presumably caused by a very small (~1%) difference between $3/^1J_{C^\varepsilon H^\varepsilon}$ and the duration T + 2ξ. As anticipated, Met[51] and Met[145], which have a high population of the $\chi^3 = 180°$ rotamer, exhibit the weakest $^3J_{C^\varepsilon H^\gamma}$ couplings (Table 1). As mentioned above, Met[76] is highly flexible and the Met[76] $^3J_{C^\varepsilon H^\gamma}$ values are believed to be representative for a disordered methionine residue. For residues with a χ^3 angle of either +60° or −60°, a large $^3J_{C^\varepsilon H^\gamma}$ value would be expected for only one of the H^γ methylene protons. However, for most of the residues with $\chi^3 \neq 180°$ the two $^3J_{C^\varepsilon H^\gamma}$ have values in the 5–6 Hz range, suggesting that rotameric averaging occurs. Except for the correlations observed for Met[145], the intensity ratios from which the J values were derived agree remarkably well with those observed in an 8 h experiment, recorded with T = 19.4 ms (data not shown). Based on this
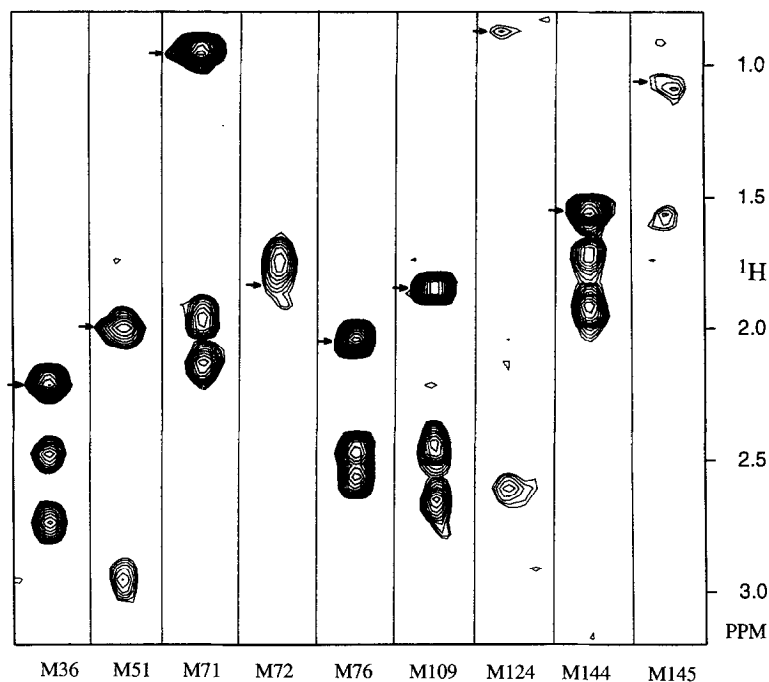

Fig. 7. F_1 strip plot of the 3D LRCH spectrum of the calmodulin–M13 complex, showing the correlation between C^ε/H^ε and H^γ resonances for the methionine residues. Spurious diagonal resonances ($F_1 = F_3 = \delta H^\varepsilon$) are marked by arrows. Contours are spaced exponentially by $2^{1/3}$.

TABLE 1

RESONANCE ASSIGNMENTS AND J COUPLINGS FOR VARIOUS SIDE-CHAIN RESONANCES OF METHIONINE RESIDUES IN THE CALMODULIN–M13 COMPLEX[a]

	C^β	C^γ	$H^{\gamma'}$	$H^{\gamma''}$	C^ε	H^ε	$^3J_{C^\varepsilon C^\beta}$	$^2J_{C^\varepsilon C^\gamma}$	$^3J_{C^\varepsilon H^{\gamma'}}$	$^3J_{C^\varepsilon H^{\gamma''}}$
Met[36]	31.2	33.5	2.74	2.48	18.2	2.21	1.1	0.6	6.1	4.7
Met[51]	33.3	33.5	2.97	2.92	18.4	2.01	2.0[b]	–	3.5[e]	3.5[e]
Met[71]	31.9	32.0	2.14	1.97	17.3	0.97	0.8[b]	–	6.1	5.4
Met[72]	29.5	31.1	1.79	1.71	15.0	1.86	0.6	0.6	[g]	large[h]
Met[76]	33.7	32.4	2.56	2.47	17.2	2.04	0.8	0.5	5.8	6.6
Met[109]	32.6	32.4	2.66	2.44	18.2	1.86	0.5[c]	0.5[c]	5.5	6.7
Met[124]	33.0	32.9	2.61	–	15.4	0.89	0.6[c]	0.6[c]	6.6[f]	<3.8[d,f]
Met[144]	30.8	30.9	1.92	1.72	16.7	1.57	0.6[c]	0.6[c]	7.3	5.8
Met[145]	30.4	32.5	1.58	0.91	18.8	1.09	2.2	≤0.5[d]	4.5	3.2

[a] Chemical shifts are for a complex between genetically engineered *Drosophila* calmodulin, lacking posttranslational modifications, complexed with one equivalent of the M13 peptide (Klevit et al., 1984). Chemical shifts are in ppm, relative to TSP.

[b] The J value has been calculated by subtracting the intensity expected for the overlapping two-bond correlation, based on $^2J_{C^\varepsilon C^\gamma} = 0.5$ Hz, from the observed intensity prior to calculating $^3J_{C^\varepsilon C^\beta}$.

[c] We assume that the two- and three-bond correlations contribute equally to the cross peaks (C^β and C^γ overlap).

[d] Upper limit, based on the absence of intensity.

[e] We assume that correlations to $H^{\gamma'}$ and $H^{\gamma''}$ contribute equally.

[f] We assume that $H^{\gamma''}$ does not overlap with $H^{\gamma'}$.

[g] $H^{\gamma'}$ overlaps with H^ε.

[h] Partial overlap.

observation, it is estimated that the random error in $^3J_{C^\varepsilon H^\gamma}$ is smaller than about 0.5 Hz. Additional small systematic errors due to pulse imperfection and ^1H-^1H spin diffusion may also be present, however.

Qualitatively, the $^3J_{C^\varepsilon H^\gamma}$ and $^3J_{C^\beta C^\varepsilon}$ values reported in Table 1 agree very well with one another: The larger the $^3J_{C^\beta C^\varepsilon}$ value, the smaller the average value of $^3J_{C^\varepsilon H^\gamma}$. For quantitative assessment of the rotamer populations, the ^3J values for the individual rotamers need to be known. Unfortunately, the literature for three-bond J couplings through sulfur is rather scarce, and no good Karplus relations are available (Krivdin and Della, 1991). The largest $^3J_{CC}$ values measured in the present case are substantially smaller than values measured for trans $^3J_{CC}$ couplings to methyl carbons in other protein residues (~3.5 Hz), but it remains uncertain whether this is due to rotamer averaging or to the presence of the sulfur atom in the coupling pathway.

CONCLUSIONS

The methods described above permit unambiguous assignment of the methionine $C^\varepsilon H_3$ resonances in the complex between calmodulin and a target peptide. With the exception of residues Met[72], Met[124] and Met[145], which are subject to line broadening caused by slow conformational averaging, the sensitivity of the experiments described above is high. The experiments also yield $^3J_{C^\varepsilon H^\gamma}$ and $^3J_{C^\beta C^\varepsilon}$ values, thereby providing information on the χ^3 angle of methionine residues, which frequently play an important role in protein–protein interactions.

ACKNOWLEDGEMENTS

REFERENCES

Bax, A. and Pochapsky, S.S. (1992) *J. Magn. Reson.*, **99**, 638–643.

Bax, A. and Summers, M.F. (1986) *J. Am. Chem. Soc.*, **108**, 2093–2094.

Bax, A., Clore, G.M. and Gronenborn, A.M. (1990) *J. Magn. Reson.*, **88**, 425–431.

Bax, A., Max, D. and Zax, D. (1992) *J. Am. Chem. Soc.*, **114**, 6924–6925.

Cohen, P. and Klee, C.B. (1988) *Molecular Aspects of Cellular Regulation*, Vol. 5, Elsevier, New York, NY.

Fesik, S.W., Eaton, H.L., Olejniczak, E.T., Zuiderweg, E.R.P., McIntosh, L.P. and Dahlquist, F.W. (1990) *J. Am. Chem. Soc.*, **112**, 886–888.

Finn, B.E., Drakenberg, T. and Forsen, S. (1994) *FEBS Lett.*, **336**, 368–374.

Grzesiek, S. and Bax, A. (1992) *J. Magn. Reson.*, **99**, 201–207.

Ikura, M., Clore, G.M., Gronenborn, A.M., Zhu, G., Klee, C.B. and Bax, A. (1992) *Science*, **256**, 632–638.

Kay, L.E., Ikura, M. and Bax, A. (1990) *J. Am. Chem. Soc.*, **112**, 888–889.

Klevit, R.E., Dalgarno, D.C., Levine, B.A. and Williams, R.J.P. (1984) *Biochemistry*, **24**, 8152–8157.

Kretsinger, R. (1992) *Cell Calcium*, **13**, 363–376.

Krivdin, L.B. and Della, E.W. (1991) *Prog. NMR Spectrosc.*, **23**, 301–610.

Marion, D., Ikura, M., Tschudin, R. and Bax, A. (1989) *J. Magn. Reson.*, **85**, 393–399.

Meador, W.E., Means, A.R. and Quiocho, F.A. (1992) *Science*, **257**, 1251–1255.

Meador, W.E., Means, A.R. and Quiocho, F.A. (1993) *Science*, **262**, 1718–1721.

O'Neil, K.T. and DeGrado, W.F. (1990) *Trends Biochem. Sci*, **15**, 59–64.

Santoro, J. and King, G.C. (1992) *J. Magn. Reson.*, **97**, 202–207.

Van de Ven, F.J.M. and Philippens, M.E.P. (1992) *J. Magn. Reson.*, **97**, 637–644.

Vuister, G.W. and Bax, A. (1992) *J. Magn. Reson.*, **98**, 428–435.

Vuister, G.W. and Bax, A. (1993) *J. Magn. Reson. Ser. B*, **102**, 228–231.

Vuister, G.W., Yamazaki, T., Torchia, D.A. and Bax, A. (1993) *J. Biomol. NMR*, **3**, 297–306.

Vuister, G.W., Grzesiek, S., Delaglio, F., Wang, A.C., Tschudin, R., Zhu, G. and Bax, A. (1994) *Methods Enzymol.*, **239**, 79–105.

Zhu, G. and Bax, A. (1990) *J. Magn. Reson.*, **90**, 405–410.

Zhu, G. and Bax, A. (1993) *J. Magn. Reson. Ser. A.*, **104**, 353–357.